

# Aerodynamic Drag of Streamers and Flags

A. C. Carruthers\* and A. Filippone†

*The University of Manchester, Manchester, England M60 1QD, United Kingdom*

Low-speed drag and flutter measurements of rectangular flags and streamers are presented. The streamers have aspect ratios between 10 and 30; the flag has an aspect ratio of 3.3. Operating Reynolds numbers are in the range from  $Re = 2 \times 10^5$  to  $2 \times 10^6$ . Experiments are performed with three fabrics of different weight, bending rigidity, and hysteresis. The streamers are fixed to a three-component force balance by the use of two methods: by clamping of the luff on the support and by a wire connecting luff and support. The parametric space studied includes wind speed, aspect ratio, planform area, clamping method, and fabric properties. Semi-empirical correlations for the time-averaged drag coefficient as a function of aspect ratio are derived for cotton streamers. Flutter analysis shows that the oscillation of the streamers is complex due to the effects of gravity and the turbulence created by the large-amplitude oscillations. Power spectra density data are presented for some relevant cases.

## Nomenclature

$A$	=	reference area, $\text{g/m}^2$
$\mathcal{R}$	=	aspect ratio
$C_D$	=	drag coefficient
$D$	=	drag force, N
$l$	=	reference length, m
$Re$	=	Reynolds number
$Re_c$	=	critical Reynolds number
$u$	=	wind speed, m/s
$W$	=	weight

## Introduction

THE results of wind-tunnel investigations on slender rectangular flags fixed at one end and freely moving in the vertical direction are discussed in this paper. In the technical literature, these flags are named ribbons, streamers, banners, or strips, depending on their aerodynamic applications. These applications include a number of aerodynamic decelerator systems (parachutes, cords, and parts of the canopy), stabilisers for weapon systems (rocket-launched grenades), and other purposes, for example, kites and tow bars for flying billboards. There is also interest in the wind loads on flag poles caused by high winds or excessively large flags, or as a source of drag (when high drag is desirable).

Two types of attachment are possible, with streamers tied at one or both ends; in the latter case, they are known as tapes. However, only the former case is considered here. For clarity, the term flag is adopted in our discussion when the aspect ratio is modest (less than 4). The term streamer will be used in all other cases.

For configurations where horizontal mounting is used, the gravity has a more significant effect. In fact, for a streamer attached at one end on a horizontal line, the aerodynamic forces work against the gravity and create additional instabilities. Flutter analysis is difficult even in laminar flow.

Modern applications include technological materials, such as polyester, nylon, Mylar®, Kevlar®, and others, but experimental data in this field are surprisingly scarce. Some drag data were published as early as 1930 by Fairthorne,<sup>1</sup> in response to the need of data

for advertising streamers towed by aircraft. The data reported by this author were for rectangular flags of aspect ratio 0.5–4.0 and triangular flags of aspect ratio 0.25–1.0. The data showed the following: 1) The drag coefficient decreased with increasing aspect ratio. 2) The nonviscous drag component depended on the mass of the fabric. Reference 2 an important resource for drag characteristics in all fields of engineering, contains little data on this type of study and is not specific as to which reference area was used to present the data. Hoerner himself referred to the work of Fairthorne and reported only drag data for ordinary low aspect ratio flags.

More recently, Levin et al.<sup>3</sup> published drag data for eight different types of materials, characterized by their weight (per unit length). The streamers were fixed at the trailing edge of a symmetric airfoil and free to move in the vertical direction. The aspect ratios tested were in the range between 2 and 22. The results showed how the drag coefficient decreases with the increasing aspect ratio, as a consequence of the axial force increasing with the amplitude of fluctuation of the free edges. These authors also discussed dynamic tests aimed at describing the effects of fluttering. This fluttering produced (obviously) more scattered results than static tests. This conclusion has been confirmed by the present study.

Auman and Dahlke<sup>4</sup> investigated the drag of “ribbonis” used for reducing the hazardous dud rate of rocket-launched grenades. Aspect ratios tested were in the range from 4 to 75, and speeds tested were from subsonic to supersonic (Mach number  $\sim 2$ ), although the data were not presented as a function of the Reynolds number (based on the length of the streamers). Some of these tests were made with a grenade gun. It was proved that, for a flight vehicle, the slender ribbons work as stabilisers, although several flight characteristics of the grenade were detected.

The stability problem of the flags was investigated earlier by Taneda,<sup>5</sup> who studied the waving motion of flags at relatively low speeds ( $Re = 10^4$ – $10^5$ ). Oscillation modes and limits of stability were discussed, and a Strouhal number for the oscillations was derived. Taneda implied that the flutter frequency was unique and that it increased with the wind speed, but this is unlikely to be the case. Furthermore, it was proved that the drag coefficient at a given Reynolds number depends on whether the flag is fluttering or not. The critical Reynolds number at which the flag reverts to a fluttering mode ( $Re_c \sim 10^4$ ) also creates a jump in the drag coefficient that is justified by flow separation and by momentum transfer to the flow during oscillations. Taneda’s experimental setup included vertical flags in a vertical wind-tunnel flow, which eliminated most of the gravity effects. The drag of the flags, in fact, acts in the same direction as the weight, and in the laminar or transitional Reynolds numbers, the flutter characteristics are relatively simple.

Methods for theoretical modeling of flags and streamers are rare in the technical literature, except for some computer graphics applications that are not based on physics. The experimental data reported by the authors cited are generally described by the use of

Received 2 April 2004; revision received 10 June 2004; accepted for publication 30 June 2004. Copyright © 2004 by A. Filippone. Published by the American Institute of Aeronautics and Astronautics, Inc., with permission. Copies of this paper may be made for personal or internal use, on condition that the copier pay the \$10.00 per-copy fee to the Copyright Clearance Center, Inc., 222 Rosewood Drive, Danvers, MA 01923; include the code 0021-8669/05 \$10.00 in correspondence with the CCC.

\*Graduate Student, Department of Mechanical, Aerospace, and Civil Engineering, Student Member AIAA.

†Lecturer, Department of Mechanical, Aerospace, and Civil Engineering; a.filippone@manchester.ac.uk. Senior Member AIAA.

semi-empirical expressions. This is also the approach followed in the present study.

Theoretical analyses of two-dimensional flags in potential flow model exist, with focus on flutter, tension, modes of oscillation, and stability. Sparenberg<sup>6</sup> modeled the waving motion of a membrane and derived an equation for the flapping frequency, assuming a Kutta condition at the trailing edge. Moretti<sup>7</sup> studied the tension in fluttering flags under the assumption that the gravity has no effect. A study on paper flutter was published by Watanabe et al.,<sup>8</sup> in which the full Navier–Stokes equations were used for a flutter simulation. These results were compared with a potential flow analysis on an oscillating thin airfoil and showed surprising consistency between the two methods in terms of flutter modes prediction. In another study, Fitt and Pope<sup>9</sup> derived a theory for the unsteady motion of two-dimensional flags in a potential flow, under the assumption of small perturbations. Fitt and Pope studied the limits of stability of the flags in unsteady motion (depending on rigidity and mass) with clamped and flexible leading edges; they did not derive expressions for the drag.

Some flexible structures have been the subject of theoretical analysis by Alben et al.,<sup>10</sup> who studied the drag reduction properties of bodies with certain flexural rigidity, including the characteristics and self-similarity solutions.<sup>11</sup>

This paper fills in the technical literature with new data for streamers having clamped and flexible leading edges. The effects of the oscillations of the streamers on the resulting drag have been investigated and are discussed. An analysis has been carried out to evaluate the aspect ratio effects on the aerodynamic drag at a constant wetted area. A broad parametric space is investigated. This includes, in particular, material properties, planform area, clamping method, and aspect ratio.

Flapping frequency is also discussed in some relevant cases. It is proved that there is a complex spectrum of flutter frequencies and that frequency separation is not possible.

### Experimental Setup

A wind tunnel of working section  $0.9 \times 0.9$  m, 3.14 m long, incorporating an externally mounted three-component force balance, was used to take the drag measurements. There were 12 streamers of cotton fabric made, with planform areas  $0.025$  m<sup>2</sup>,  $0.05$  m<sup>2</sup>, and  $0.075$  m<sup>2</sup>. For each of these streamers, four aspect ratios were considered: 3.3, 10, 20, and 30.

Additional tests were carried out with two other materials. These tests involved both nylon with one-side polyurethane coating and polyester with geometries  $\mathcal{AR} = 10$  and  $A = 0.025$  m<sup>2</sup> and  $\mathcal{AR} = 20$  and  $A = 0.05$  m<sup>2</sup>, respectively. An additional streamer with  $\mathcal{AR} = 30$  and  $A = 0.075$  m<sup>2</sup> was made of polyester. The edges of all streamers were painted with a water and polyvinyl acetate glue (PVA) adhesive mixture and were subsequently burned to prevent or reduce fraying.

A third set of experiments involved two different methods to mount the streamers: clamped and free luff. (The luff is the edge of the streamer facing the wind.) For both methods, eyelets were punched in the luff corners of each streamer and were then used to secure each mounting method. The arrangement is shown in Fig. 1. The clamped streamer configuration had each eyelet fastened di-

rectly to holes in the mounting rod (with 6-mm diameter), such that the luff was pulled taut. The eyelets were fastened via small pieces of flexible wire, the ends of which were taped to the upstream side of the rod to minimize any aerodynamic effect. The free streamer configuration also had the leading edge pulled taut by a thin piece of rigid wire, the center of which was attached to the mounting rod via a length of 120-mm flexible wire. Again, the free ends of the wire, once tied, were taped to the mounting rod upstream side. The streamers tested in these experiments were nylon and polyester streamers of  $\mathcal{AR} = 10$  and area  $A = 0.025$  m<sup>2</sup>, nylon and polyester streamers of  $\mathcal{AR} = 20$  and area  $A = 0.05$  m<sup>2</sup>, and cotton and polyester streamers of  $\mathcal{AR} = 30$  and area  $A = 0.075$  m<sup>2</sup>.

Therefore, a combination of planform areas and aspect ratios were tested over a range of wind speeds to produce a matrix of drag data that have ultimately made possible the comparison of planform areas, aspect ratios, materials, and wind speeds. The drag of the support rod was subtracted from the drag force measured by the balance. A list of the streamers' configurations is given in Table 1.

The drag coefficient was calculated based on the planform area of each streamer. Reynolds numbers were calculated based on each streamer length and the freestream velocity. A velocity range from 6 to 18 m/s was investigated, measured with a pitot static probe in the wind tunnel. The probe connected to a high-accuracy digital manometer that measured to within 0.01 mm H<sub>2</sub>O (0.098 Pa).

Measurements were taken with a force balance through which a mounting rod was secured. A time series was taken for each data point, 2048 samples over 2 s, and averaged to give a mean drag measurement. This voltage output was converted to a force measurement through a calibration curve, obtained by the application of forces to the force balance center. A vibration unit was connected through the balance and used immediately before readings were taken to reduce sticktion through the force balance collet. For each respective streamer setup, the final results were averaged over a set of nine tests, three obtained on each of three separate days.

Table 2 shows the bending rigidity of the fabric, which is its stiffness, for example, resistance to deformations, and the bending hysteresis, which characterizes its recovery after deformation. The higher is the bending hysteresis, the poorer is the recovery of the fabric. Note that the weight of the cotton fabric is roughly three times the weight of polyester and 20% higher than the weight of nylon. On the other hand, the bending rigidity of nylon is nearly one order of magnitude larger than the cotton.

**Table 1 Streamers and flags tested**

$\mathcal{AR}$	Length, m	Width, m
<i>Area = 0.025 m<sup>2</sup></i>		
3.3	0.287	0.087
10.0	0.500	0.050
20.0	0.707	0.035
30.0	0.866	0.029
<i>Area = 0.050 m<sup>2</sup></i>		
3.3	0.406	0.123
10.0	0.707	0.071
20.0	1.000	0.050
30.0	1.225	0.041
<i>Area = 0.075 m<sup>2</sup></i>		
3.3	0.498	0.151
10.0	0.866	0.087
20.0	1.225	0.061
30.0	1.500	0.050

**Table 2 Material properties of streamers tested**

Material	Weight, g/m <sup>2</sup>	Bending rigidity, g · cm <sup>2</sup> /cm	Bending hysteresis, g · cm/cm	$\mathcal{AR}$	Area, m <sup>2</sup>
Cotton	177	0.0642	0.0446	All	All
Nylon <sup>a</sup>	140	0.4795	0.2103	10, 20	0.025, 0.05
Polyester	64	0.1313	0.0419	10, 20, 30	0.025, 0.05, 0.075

<sup>a</sup>Nylon fabric had a polyurethane coating on one side.

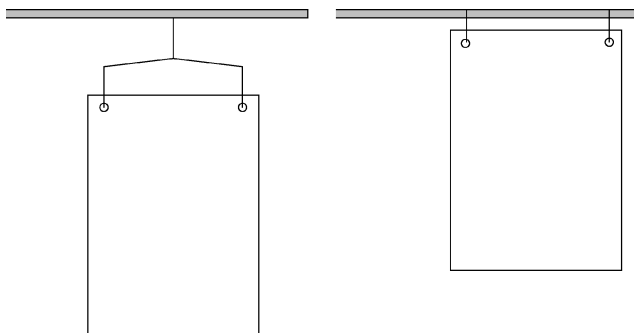


**Fig. 1 Free and clamped mounting methods by flexible wire, mounting rod horizontal in wind-tunnel section.**

All streamers were damaged during testing to some extent, particularly at the highest speeds, when the streamers underwent small-amplitude oscillations and high-frequency oscillations. The smaller-amplitude oscillations are confined to the leech as the wind speed is increased. (The leech is the downstream or trailing edge of the streamer.) The streamers having the lowest aspect ratio ( $AR = 10$ ) suffered the least damage, with at most one or two fibers breaking loose. This minor damage had a negligible effect on the drag data, and it could be ignored. The longest streamers ( $AR = 30$ ) suffered more notable fraying. In these cases, up to 3 mm of the streamer leech became frayed, and up to one-quarter of the streamer lengths edges were affected, with fibers breaking loose as was the case with the lower aspect ratio test. The damage during testing was considered to be little enough that new streamers were only introduced for each of the mounting methods, and, consequently, only two of each of these streamers, smooth (polyester) and rough (cotton or nylon) for  $AR = 20$  and 30, were made.

Additional tests were carried out without a PVA/water edging, to determine the effects on the measurements being carried out. Over a short time interval, the streamers incurred notable damage. When the damage was negligible, the drag results compared well to those with the mixture edging. It was concluded that the method used to seal the streamer edges left the drag characteristics unchanged.

## Results and Discussion

The results are presented as a function of the Reynolds number or the wind speed. The wind speed was chosen to compare the drag coefficients of different aspect ratios because the Reynolds number effect tends to shift the data apart.

The drag coefficient was calculated with the projected area of one side of the streamer used as a reference area (Fig. 2). Data presented elsewhere, for example, in Ref. 4, are derived with the total wetted area, which is twice as large. (Therefore, the  $C_D$  would be one-half as large.)

Error bars are included in all of the experimental data. For clarity, some of the error bars have been removed; error bars have been plotted either at the extreme values of the wind speed/Reynolds number, or at specified distances between data samplings, generally 5% of the graph size. The error bars give an indication of the repeatability of the tests and the unsteadiness of the aerodynamic forces due to flapping and self-induced turbulence. This factor was not clearly emphasized in the literature that we have reviewed.

The amplitude of the error bar was calculated from the minimum and maximum deviation with respect to the mean value of nine records taken at each operation point. In the results discussed hereafter, only the error bars on the  $C_D$  were plotted because the error bar on the Reynolds number or the wind speed was negligible. In most cases, the error bar on the  $C_D$  of the free streamers is considerably larger than the corresponding error bar on the clamped streamer, all other parameters being the same. This is attributed to the additional degree of freedom of the streamer in the wind tunnel.

### Drag of Cotton Streamers

Figures 3–5 show the relationship between drag and aspect ratio for the cotton fabric over the full range of velocities tested. The trend lines through each of the three data sets are similar. The curve trend

for the largest planform area is

$$C_D = 0.405AR^{-0.494} \quad (1)$$

The curve for the lowest planform area is

$$C_D = 0.561AR^{-0.480} \quad (2)$$

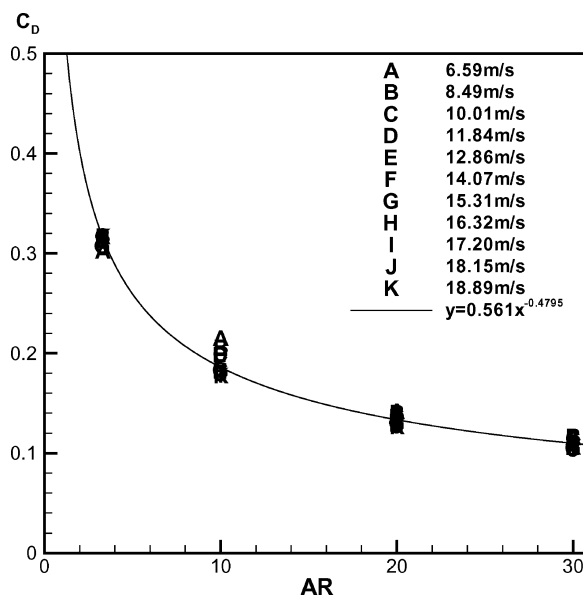


Fig. 3 Drag coefficient trends at constant planform area  $A = 0.025 \text{ m}^2$  for cotton streamers and correlation with power curve, fixed mounting.

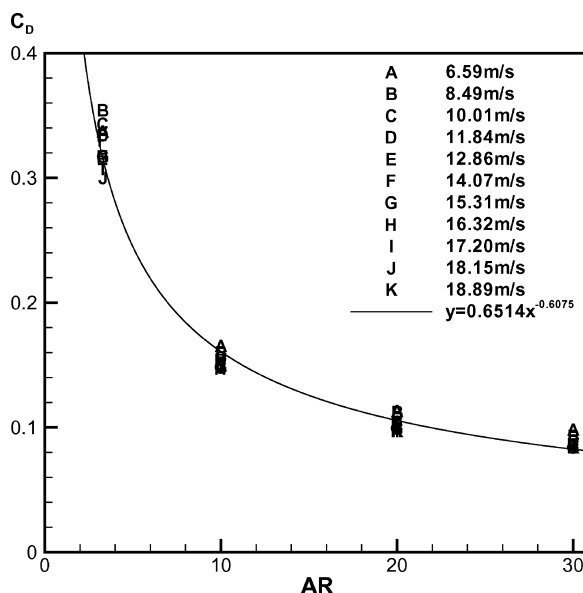


Fig. 4 Drag coefficient trends at constant planform area  $A = 0.05 \text{ m}^2$  for cotton streamers and correlation with power curve, fixed mounting.

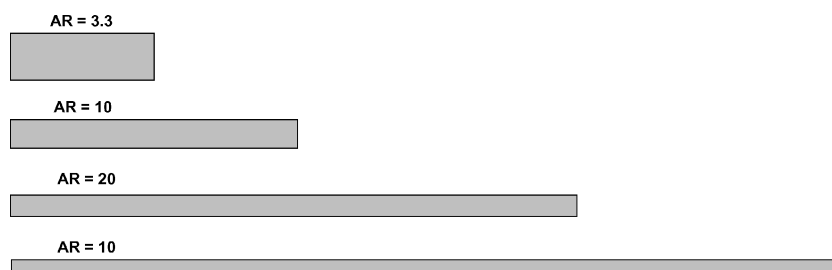


Fig. 2 Effect of aspect ratio on streamers tested.

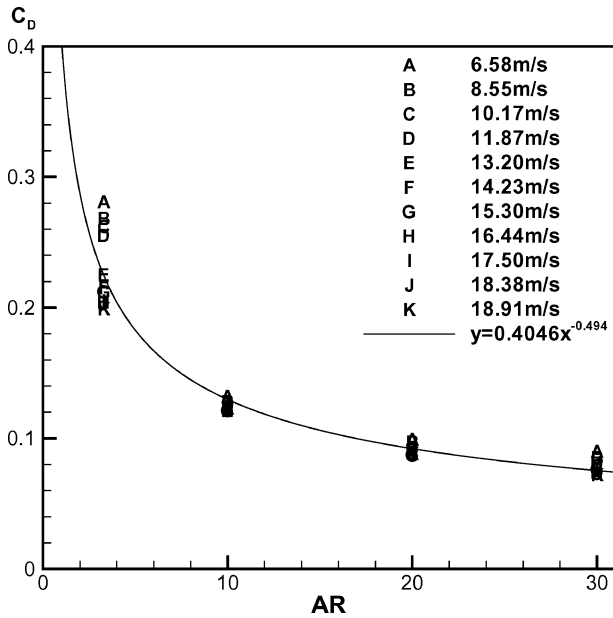


Fig. 5 Drag coefficient trends at constant planform area  $A = 0.075 \text{ m}^2$  for cotton streamers and correlation with power curve, fixed mounting.

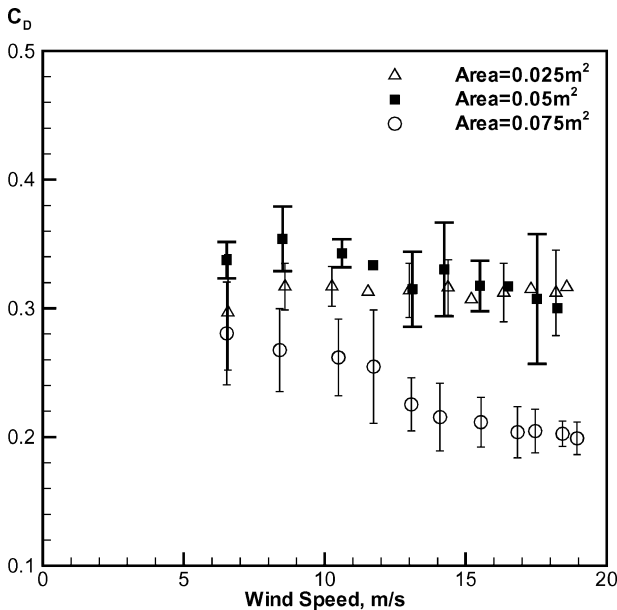


Fig. 6 Effects of planform area on  $C_D$ , flag  $AR = 3.3$ , fixed mounting.

The present curve fit is very close to the experimental data of Auman and Dahlke<sup>4</sup> when the  $C_D$  is calculated with reference to the total wetted area. Even when aspect ratios larger than the ones tested are considered, the correlation is excellent.

The data show that the effect of aspect ratio is far larger than the effect of wind speed for a given planform area. Note, however, that at the lowest aspect ratio ( $AR = 3.3$ ) there is a relatively large scatter of data for higher planform areas, Figs. 4 and 5. In particular, there is a jump in the drag levels of the flag with the planform area  $A = 0.075 \text{ m}^2$ , with data clustered around two main areas.

Figures 6–9 show the effects of planform area on the drag coefficient as a function of the wind speed for cotton flags and streamers. These are the data points in the graphics of Figs. 3–5.

The details of the flag data are shown in Fig. 7. For the largest planform area, two distinct drag levels are observed. At the low-speed range,  $u = 6\text{--}12 \text{ m/s}$ , the drag level is weakly dependent on the speed. At the upper end of this band, corresponding to a Reynolds number  $Re \sim 7.2 \times 10^5$ , an abrupt drag change occurs. This is attributed to a change in oscillation mode. The higher drag encountered at low speed is due to larger volume of air being disturbed in

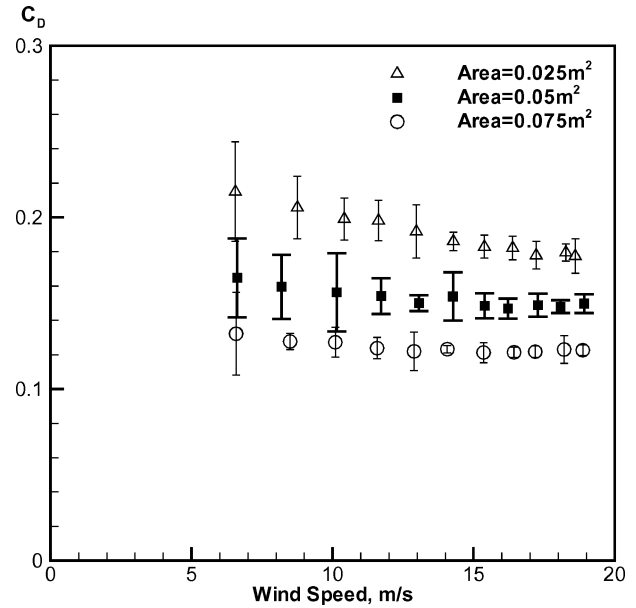


Fig. 7 Effects of planform area on  $C_D$ , streamer  $AR = 10$ , fixed mounting.

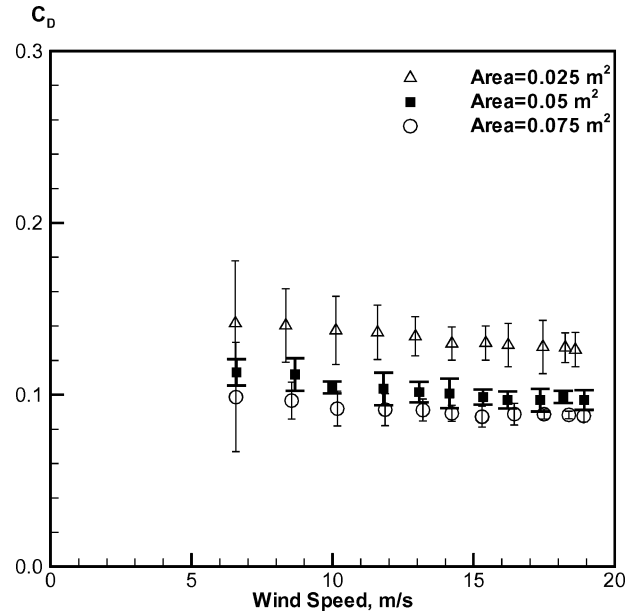


Fig. 8 Effects of planform area on  $C_D$ , streamer  $AR = 20$ , fixed mounting.

the flapping movement of the flag. These flags oscillate with high amplitude and low frequencies at low wind speeds; the amplitudes decrease and the frequencies increase with increasing wind speed.

The value of the Reynolds number  $Re = 7.2 \times 10^5$  is achieved at the largest speed with a flag of planform area  $A = 0.05 \text{ m}^2$ . No clear drag crisis is evident in this case, although the data are more erratic than in other cases.

It is observed that the smallest area produced the highest drag; the largest area produced the lowest drag. This is due to the velocity range over which the large-amplitude, low-frequency oscillations take place. At the lowest velocities, the smallest areas catch in the wind speed, thereby producing a high-amplitude, lower-frequency oscillation. However, the streamers having larger area are too long and heavy, and only at a higher speeds are they able to catch the wind. Each streamer area displays high-amplitude, low-frequency oscillations at low speed, and low-amplitude, high-frequency oscillations at high speed. However, the smaller streamers, being shorter and lighter, suffer a more violent oscillation at all speeds. Indeed, the side-to-side rotational movement is notably more violent for the

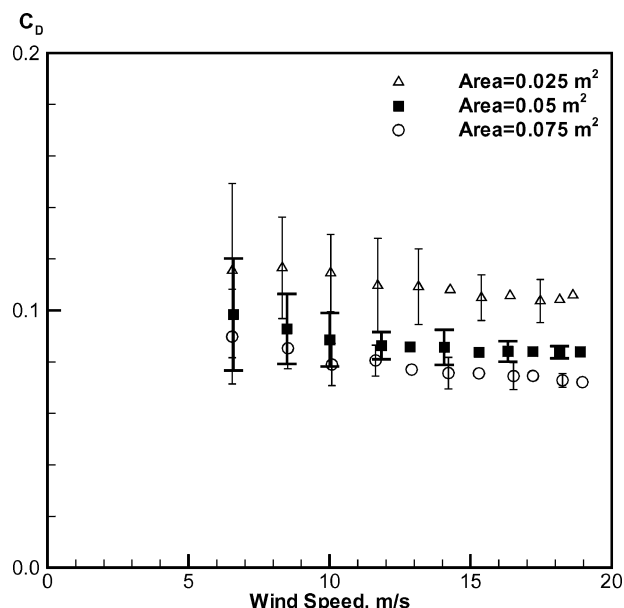


Fig. 9 Effects of planform area on  $C_D$ , streamer  $AR=30$ , fixed mounting.

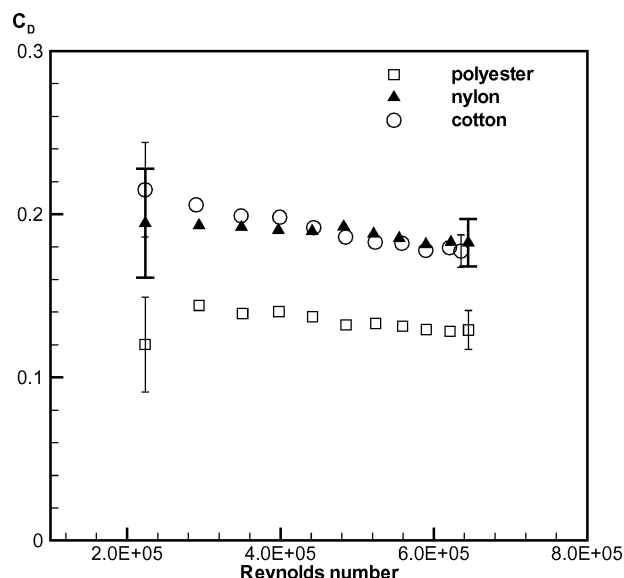


Fig. 10 Effects of fabric type on  $C_D$ ,  $AR=10$ ,  $A=0.025 \text{ m}^2$ , fixed mounting.

lower areas and, in relation to their widths, is deflected by far greater amplitudes. This results in higher drag.

#### Effects of Fabric Type

In addition to the cotton experiments, two other fabrics were tested: nylon with poly-urethane coating on one side and polyester (Table 2), for two test cases,  $AR=10$  and  $A=0.025 \text{ m}^2$  and  $AR=20$  and  $A=0.05 \text{ m}^2$ . Drag results as a function of the Reynolds number for the three fabrics are shown in Figs. 10 and 11.

The materials have two distinctive properties that affect the aerodynamics, surface roughness, and material weight. The polyester material has the lightest weight and smoothest material. Both attributes combine to result in a significantly lowered drag compared to the other two fabrics. The cotton material is notably the heaviest and is of relatively rough weave, resulting in the highest drag characteristics.

The nylon fabric has unusual characteristics due to the single-sided coating of polyurethane that makes one side virtually as smooth as the polyester fabric and the uncoated side virtually as rough as the cotton fabric. Combined with this is a fabric weight

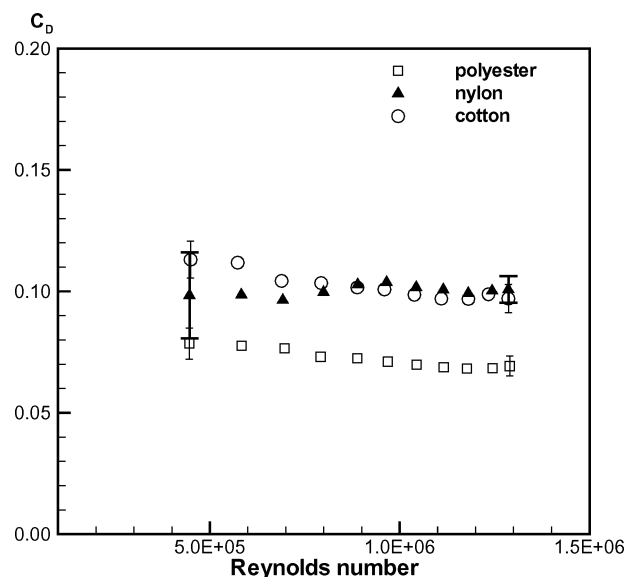


Fig. 11 Effects of fabric type on  $C_D$ ,  $AR=20$ ,  $A=0.05 \text{ m}^2$ , fixed mounting.

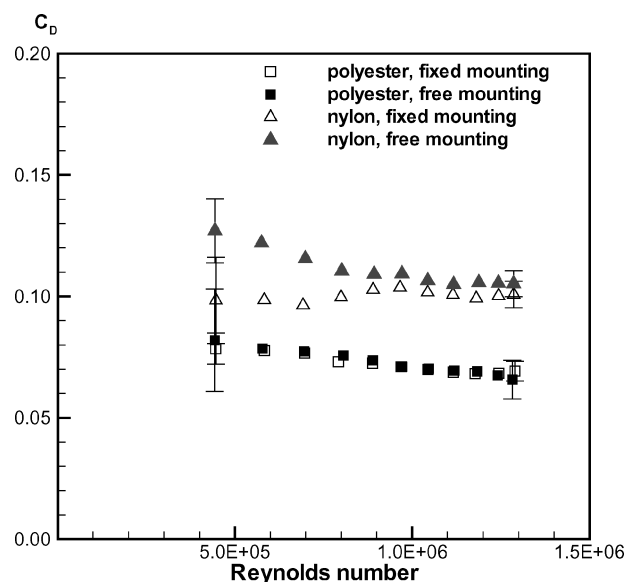


Fig. 12 Effects of mounting method,  $AR=20$ ,  $A=0.05 \text{ m}^2$ .

between that of the two other fabrics that results in drag characteristics between the two. The exception to this is at high velocities, where it becomes increasingly difficult to separate the cotton and nylon streamers, and, indeed, the drag of the nylon actually increases slightly above the drag of the cotton. This is mainly due to the bending rigidity of the nylon (Table 2), 3.5 and 7.5 times higher than cotton and polyester, respectively. Therefore, because nylon is stiffer, a drag curve that appears more constant with velocity changes is produced. At the lower velocities, when the large-amplitude oscillations occur, the material is more resistant to the incident forces, resulting in a lesser drag magnitude. As the velocity is increased and the lower-amplitude oscillations dominate, the streamer takes on a less violent motion, and the drag magnitude is not significantly altered.

#### Effects of Mounting Method

Figures 12 and 13 show the effects of the mounting method on the drag characteristics of streamers of  $AR=20$  and  $A=0.05 \text{ m}^2$  and  $AR=30$  and  $A=0.075 \text{ m}^2$ . Note that, as with the clamped mounting method comparison, the polyester has lower drag than both cotton and nylon fabrics for both mounting methods.

The higher drag produced with the free mounting method is expected because an increased volume of air is affected by the flow

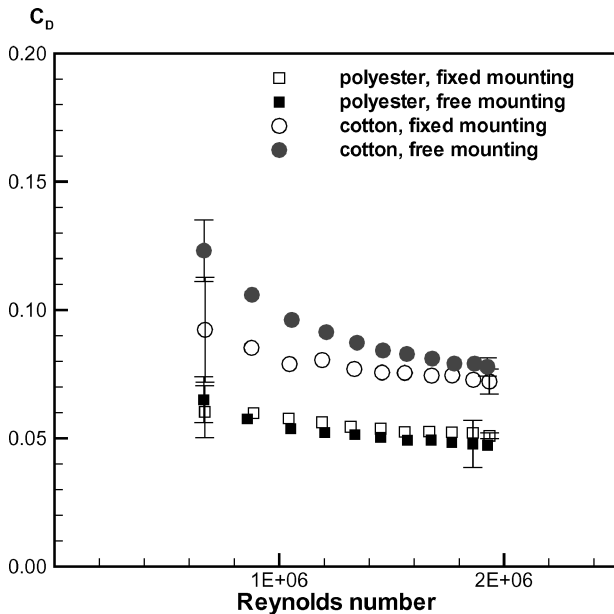


Fig. 13 Effects of mounting method,  $AR = 30$ ,  $A = 0.075 \text{ m}^2$ .

perturbation. The streamer is, in fact, allowed to move, but with relative freedom of movement at the luff. This results in increased rotational movement because completed revolutions of the streamer are allowed. Hence, a larger drag is created through this additional degree of freedom.

Thus, at lower velocities, the large-amplitude oscillations are given relative freedom to move, which creates a more violent flow than that observed with the clamped mounting method and results in a widened drag deviation from the clamped mounting method. At higher velocities, whereas the streamer is pulled out flat while experiencing the low-amplitude oscillations, the extra freedom of movement results in a more violent motion. This results in drag magnitudes that are similar to each other, but that are slightly higher than those derived with the clamped mounting method.

The exception to this is the cotton material, which exhibits little variation between mounting methods. This is most probably due to its bending rigidity, almost one order of magnitude lower than the nylon and one-half of the value of the polyester. This results in the different mounting method having little effect on the drag. However, the nylon and polyester fabrics have a more notable difference between mounting methods because of their significantly larger bending rigidity. This means that when the free clamping method is used the streamers have significantly more movement, an effect diminished in the case of cotton by its low bending rigidity.

#### Modes of Oscillation

Two flapping modes were observed. They occur along the length of the streamer and take the form of low-frequency, high-amplitude or high-frequency, low-amplitude oscillations. The two flapping motions are not mutually exclusive, but one will instead dominate, depending on the flow conditions. At low velocities, the high-amplitude oscillations tend to dominate; at higher velocities, the lower-amplitude oscillations dominate.

A rotational movement about the streamwise axis exists for both flapping states, alternating between clockwise and anticlockwise. The rotation gives the appearance of the streamer leech (tail end) moving in a figure eight pattern.

At the lower velocity range, the streamers undergo a more violent motion than at the higher velocities due to the large-amplitude oscillations that occur periodically and can be separated visually into a set cyclical motion. The streamer would begin with a standard flapping motion as outlined earlier. The rotational movement influence then increases, so that small angles from the streamwise axis are seen in alternating positive and negative angles. As this combination of the two movements (flapping and rotational) occurs, the

balance between them shifts toward the rotational movement, and larger angles followed by complete revolutions of the streamer are observed, again in both directions. When these full revolutions occur, there appears to be higher energy in the streamer, which is then lost further downstream.

The higher energy contained within the streamers means that full revolutions can appear as bursts with significantly increased deflection from the horizontal. The energy builds up from the initial two-dimensional flapping state. The two-dimensional flapping state has the lowest-amplitude deflections and the lowest energy exchanged with the airstream.

From the rotational movements, the cycle then reverses back to the flapping movements; this is continually repeated. The number of flaps, angled flaps, and full rotations observed is dependent on the mounting method, wind velocity, streamer's aspect ratio, and material type.

#### Flutter Frequencies

Flutter frequencies have been measured with a hot wire placed in the wake of the streamers. The frequencies have been isolated by means of a fast Fourier transform. An example of power spectra density is shown in Figs. 14–16, for cotton streamers of aspect

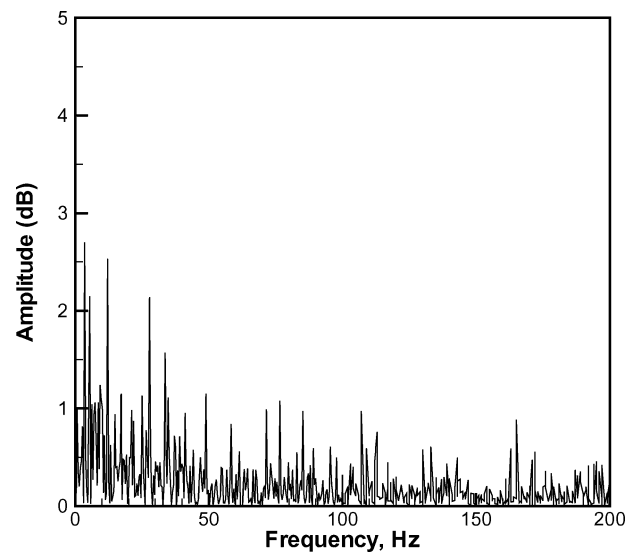


Fig. 14 Power spectra density of flutter frequency for cotton streamer  $AR = 10$ ,  $A = 0.025 \text{ m}^2$ , and  $U = 15 \text{ m/s}$ .

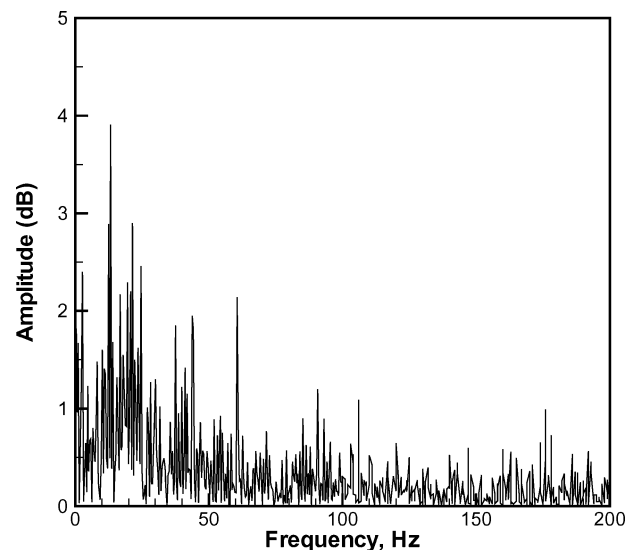


Fig. 15 Power spectra density of flutter frequency for cotton streamer  $AR = 20$ ,  $A = 0.025 \text{ m}^2$ , and  $U = 15 \text{ m/s}$ .

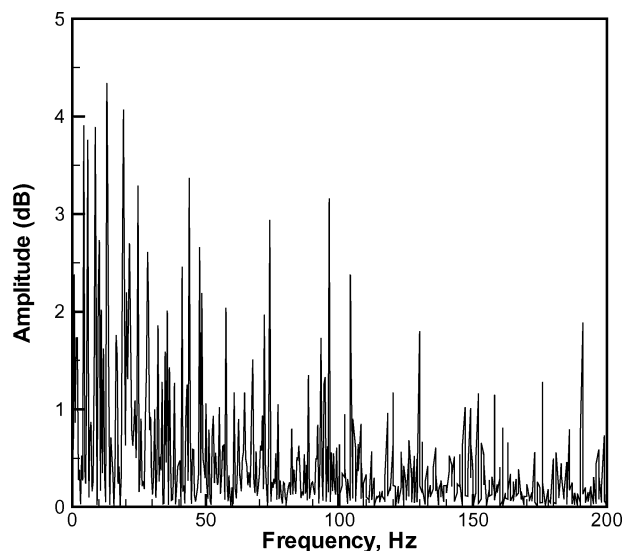


Fig. 16 Power spectra density of flutter frequency for cotton streamer  $\mathcal{R} = 30$ ,  $A = 0.025 \text{ m}^2$ , and  $U = 15 \text{ m/s}$ .

ratios  $\mathcal{R} = 10, 20$ , and  $30$ . The background noise is negligible in comparison with the output signal. The high level of turbulence behind the streamer is self-induced. The main flutter frequencies are in the range of  $5\text{--}30 \text{ Hz}$ . From tests of this nature, we have concluded that it is not possible to identify flutter frequencies as proposed by Taneda,<sup>5</sup> who had the advantage of flags pulled down by the gravity in a vertical wind tunnel running at subcritical Reynolds numbers, with fabrics up to four times heavier than those used in the present tests.

Our analysis shows that, for the cases in Figs. 14–16, the main frequencies are  $44 \text{ Hz}$  ( $\mathcal{R} = 10$ ),  $15 \text{ Hz}$  ( $\mathcal{R} = 20$ ), and  $13 \text{ Hz}$  ( $\mathcal{R} = 30$ ), respectively. For reference, Taneda shows a flutter frequency of about  $50 \text{ Hz}$  for a fabric of the same weight and a flag aspect ratio of about  $1$  at  $u = 15 \text{ m/s}$ , although the corresponding Reynolds number is one order of magnitude lower.

### Conclusions

Drag measurements were taken in a low-speed wind tunnel on a series of high aspect ratio streamers and low aspect ratio flags, made of three different fabrics that cover a wide spectrum of weights and surface roughnesses. The parametric space investigated included planform areas, wind speeds, and mounting methods. The characteristics can be extrapolated to fabrics of similar physical characteristics. The time-averaged drag data show the following:

1) With regard to the aspect ratio effect, the drag coefficient decreases with the increasing slenderness of the streamer (all other parameters being the same), in a significantly greater wind speed. Semi-empirical relations have been proposed to describe the set of averaged drag data.

2) With regard to the planform area effect, the drag coefficient increases with the increasing planform area for all types of streamers. This effect is due to a more rapid increase of the skin-friction drag than the decrease of the drag related to increased Reynolds number effects.

3) With regard to the mounting method effect, this effect has to be coupled with the bending rigidity and weight of the fabric. The low bending rigidity of the cotton produces a smaller difference between the free and clamped mounting methods. The method difference becomes very notable for nylon and polyester at low velocity.

4) With regard to the fabric properties effect, the drag coefficient decreases with the weight of the fabric and is further affected by properties such as roughness, bending rigidity, and hysteresis, all other parameters being constant. Note that, in the experiments described, the drag is not aligned with the gravity, which affects the results, particularly in the lower speed range.

5) With regard to the wind speed and Reynolds number effects, the drag coefficient generally decreases with increasing wind speed and Reynolds number. For cases where a critical Reynolds number is exceeded ( $Re \sim 7 \times 10^5$ ), a drag crisis occurs. However, due to the very low drag forces on balance at the lowest speeds, the error bar amplitudes increases, which poses some questions regarding the average value of the drag forces.

6) With regard to flutter modes and frequencies, the streamers have two basic flapping motions: low-amplitude, high-frequency and high-amplitude, low-frequency oscillations. There is a rotational motion that occurs alongside both flapping motions. The flutter is generally described by a complex power spectra density, whose peak frequencies lie in the range of  $5\text{--}30 \text{ Hz}$ .

### Acknowledgments

The authors thank Philip Blanco at the Department of Physics, University of San Diego, for the many useful discussions; Dennis Cooper of the University of Manchester Institute of Science and Technology (UMIST) for his invaluable technical help in the laboratory; and Alison Harvey, UMIST, for the fabric testing.

### References

- <sup>1</sup>Fairthorne, R. A., "Drag of Flags," Rept. 1345, Aeronautical Research Council ARC Repts. and Memoranda, U.K., May 1930.
- <sup>2</sup>Hoerner, S., *Fluid Dynamic Drag*, Author, Bricktown Heights, NJ, 1965, Chap. 3.
- <sup>3</sup>Levin, D., Daser, G., and Shpund, Z., "On the Aerodynamic Drag of Ribbons," AIAA Paper 97-1525, May 1997.
- <sup>4</sup>Auman, L. M., and Dahlke, C. W., "Drag Characteristics of Ribbons," *AIAA Aerodynamic Decelerator Systems Conferences*, AIAA, Reston, VA, 2001, pp. 131–136.
- <sup>5</sup>Taneda, S., "Waving Motion of Flags," *Journal of the Physical Society of Japan*, Vol. 2, No. 2, Feb. 1968, pp. 392–401.
- <sup>6</sup>Sprenberg, J. A., "On the Waving Motion of a Flag," *Proceedings of the Koninklijke Nederlandse Akademie van Wetenschappen, Series B: Physical Sciences*, Vol. 65, March 1962, pp. 378–392.
- <sup>7</sup>Moretti, P. M., "Tension in Fluttering Flags," *10th International Congress on Sound and Vibration*, KTH and the International Institute of Acoustics, July 2003.
- <sup>8</sup>Watanabe, Y., Isogai, K., Suzuki, S., and Sugihara, M. A., "Theoretical Study of Paper Flutter," *Journal of Fluids and Structures*, Vol. 16, No. 4, 2002, pp. 543–560.
- <sup>9</sup>Fitt, A. D., and Pope, M. P., "The Unsteady Motion of Two-Dimensional Flags with Bending Stiffness," *Journal of Engineering Mathematics*, Vol. 40, No. 3, 2001, pp. 227–248.
- <sup>10</sup>Alben, S., Shelley, M., and Zhang, J., "Drag Reduction Through Self-Similar Bending of a Flexible Body," *Nature*, Vol. 420, Dec. 2002, pp. 479–481.
- <sup>11</sup>Zhang, J., Childress, S., Libchaber, A., and Shelley, M., "Flexible Filaments in a Flowing Soap Film as a Model for One-Dimensional Flags in a Two-Dimensional Wind," *Nature*, Vol. 408, Dec. 2000, pp. 835–839.